

Cell Reports

Supplemental Information

Itraconazole Inhibits Enterovirus Replication by Targeting the Oxysterol-Binding Protein

Jeroen R.P.M. Strating, Lonneke van der Linden, Lucian Albuлесcu, Joëlle Bigay, Minetaro Arita, Leen Delang, Pieter Leyssen, Hilde M. van der Schaar, Kjerstin H.W. Lanke, Hendrik Jan Thibaut, Rachel Ulferts, Guillaume Drin, Nina Schlinck, Richard W. Wubbolts, Navdar Sever, Sarah A. Head, Jun O. Liu, Philip A. Beachy, Maria A. De Matteis, Matthew D. Shair, Vesa M. Olkkonen, Johan Neyts, and Frank J.M. van Kuppeveld

SUPPLEMENTAL INFORMATION TO:

Itraconazole inhibits enterovirus replication by targeting the oxysterol-binding protein (OSBP)

Jeroen R.P.M. Strating[®], Lonneke van der Linden[®], Lucian Albuлесcu[®], Joëlle Bigay, Minetaro Arita, Leen Delang, Pieter Leyssen, Hilde M. van der Schaar, Kjerstin H.W. Lanke, Hendrik Jan Thibaut, Rachel Ulferts, Guillaume Drin, Nina Schlinck, Richard W. Wubbolts, Navdar Sever, Sarah A. Head, Jun O. Liu, Philip A. Beachy, Maria A. De Matteis, Matthew D. Shair, Vesa M. Olkkonen, Johan Neyts, Frank J.M. van Kuppeveld

SUPPLEMENTAL EXPERIMENTAL PROCEDURES

Cell culture

Buffalo green monkey (BGM) kidney cells, HeLa R19 cells, and rhabdomyosarcoma RD cells were grown at 37°C, 5% CO₂ in DMEM Ready Mix (PAA) containing 10% fetal bovine serum or in DMEM (Lonza) supplemented with 10% fetal bovine serum. Vero, HeLa H and BGM cells used in the multicycle antiviral assays were grown in MEM supplemented with 10% FCS (Integro), 2 mM L-glutamine and 20 mM HEPES. HAP1 cells (Carette et al., 2011) (provided by Thijn Brummelkamp, NKI, Amsterdam, The Netherlands) were grown in IMDM supplemented with 10% fetal bovine serum.

Antibodies

Primary antibodies used are rabbit polyclonal anti-PI4-Kinase β antibody (Upstate), mouse monoclonal anti-PI4P antibody (Echelon Bioscience), rabbit polyclonal anti-CVB3 3A (Wessels et al., 2006), mouse monoclonal anti-CVB3 3A (Dorobantu et al., 2014), and affinity-purified rabbit polyclonal anti-human OSBP (gene ID: 5007). Secondary antibodies were Alexa Fluor 488- or 594-conjugated goat-anti-rabbit IgG or Alexa Fluor 594-conjugated goat-anti-mouse IgM (Molecular Probes).

Plasmids

Plasmids for the mammalian expression of FAPP1-PH-GFP (provided by T. Balla, NICHD, National Institutes of Health, Bethesda, Maryland, USA) (Balla et al., 2005) and rabbit OSBP pcDNA4-His-Max-rOSBP (Suchanek et al., 2007) have been previously described.

To produce plasmid pEGFP-hOSBP for mammalian expression of human OSBP with an N-terminal EGFP-tag the human OSBP cDNA (NM_002556.2) was amplified by PCR and inserted in the BamHI site of pEGFP-C1 (Clontech/Takara Bio). To produce plasmid pcDNA4-His-Max-ORP4L for mammalian expression of human ORP4L/OSBP2 with N-terminal His- and Xpress-tags the human ORP4L/OSBP2 cDNA (NM_030758) was amplified by PCR and inserted in the XbaI site of pcDNA4/HisMax C (Invitrogen).

A plasmid for the mammalian expression of human OSBP with an N-terminal EGFP-tag and a C-terminal Strep-tagII for affinity purification (GFP-hOSBP-SII) was produced by amplifying OSBP by standard PCR using a reverse primer that encoded a human codon-optimized Strep-tagII and cloning it into the Sall and BamHI sites of pEGFP-C1.

Viruses

CVB3 and CVB3-RLuc, which contains the *Renilla* luciferase gene upstream of the capsid coding region, and the 3A[H57Y] mutants of both viruses were obtained by transfection of BGM cells with RNA transcripts derived from the full length infectious clones p53CB3/T7 and pRLuc-53CB3/T7 (wt or -3A[H57Y] linearized with Sall as described before (De Palma et al., 2009; Lanke et al., 2009; Van der Schaar et al., 2012; Wessels et al., 2005).

EMCV, strain mengovirus, was produced from RNA transcripts of the infectious clone pM16.1 (a generous gift from A. Palmenberg), linearized with BamHI. The luciferase-expressing RLuc-EMCV was derived from the infectious clone pRLuc-QG-M16.1 linearized with BamHI. PV pseudoviruses (TE-PV-FLuc mc), i.e., firefly luciferase-encoding PV replicons encapsidated with capsid proteins derived from PV1 (Mahoney), were prepared as reported previously (Arita et al., 2006).

Saffold virus was described previously (Zoll et al., 2009). EV68, EV70, EV71 (strain BrCr), E11 (Gregory) and CVA21 (strain Coe) were obtained from the National Institute for Public Health and

Environment (RIVM, the Netherlands). Poliovirus Sabin 1, 2, and 3 strains were obtained from the late B. Rombaut (Vrije Universiteit Brussels, Brussels, Belgium). Human rhinoviruses 2 and 14 were a kind gift of Joachim Seipelt (Medical University of Vienna, Austria). ERAV (NM11/67) was kindly provided by David Rowlands and Toby Tuthill (University of Leeds, United Kingdom). Virus titers were determined by endpoint titration according to the method of Reed and Muench and expressed as 50% cell culture infective doses (CCID₅₀).

Multicycle CPE-reduction assay

Subconfluent monolayers of the indicated cell lines seeded in 96-well plates were treated with serial dilutions of ITZ and infected with virus at the lowest MOI that resulted in full CPE within 3 days. The medium contained 2% fetal bovine serum. Subsequently, cells were incubated at 37°C for three days until complete CPE was observed in the infected and untreated virus controls. Cell viability was determined with an MTS assay by incubating the cells with AQueous One Solution Cell Proliferation Assay (Promega) and measuring the optical density of each well at 490 or 498 nm using a microplate reader. Raw optical density values were converted to percentage of untreated and uninfected cell controls after subtraction of background values obtained with virus controls. The concentration of compound that inhibits virus-induced cell death by 50% (50% effective concentration [EC₅₀]) was calculated by nonlinear regression analysis. Cytotoxicity of ITZ was assessed in a similar set-up, and 50% cytotoxic concentration (CC₅₀) values were derived from cell viability values determined with an MTS assay. Each experiment was performed at least in triplicate.

Virus infection

Subconfluent monolayers of cells seeded in 96-well plates were infected with virus at the indicated MOI. After 30 min incubation at 37°C, the virus was removed and fresh (compound-containing) medium was added after which the cells were incubated at 37°C for the indicated length of time. For the measurement of infectious virus particles, virus was released from the cells by three rounds of freeze-thawing and virus titers were determined by end-point dilution assay. In the case of infections with RLuc-CVB3 or RLuc-EMCV, cells were lysed at 6-7hr p.i. and *Renilla* luciferase activity was measured with the *Renilla* Luciferase Assay System (Promega) according to the manufacturer's instructions. Where indicated, a cell viability MTS assay was performed in parallel as described above.

Subgenomic replicon assays

Subgenomic replicon assays for CVB3 and PV were performed as described previously using the replicons pRib-LUC-CB3/T7 and pPV-Fluc mc (wt and 3A[A70T]) respectively (Aminev et al., 2003; Arita et al., 2009; Van Ooij et al., 2006). In these subgenomic replicons the P1 area was partially (EMCV) or completely (CVB3 and PV) replaced by the sequence encoding the firefly luciferase. Linearized plasmids of the replicon constructs or of pRLuc-QG-M16.1 (EMCV infectious clone) were *in vitro* transcribed using T7 RNA polymerase. RNA was transfected into cells using either DEAE-dextran or Lipofectamine RNAiMAX and firefly (CVB3, PV) or *Renilla* (EMCV) luciferase activity was analyzed using the Luciferase Assay System (CVB3, PV) or the *Renilla* Luciferase Assay System (EMCV) (Promega) at the indicated time points.

Hepatitis C virus antiviral assays were performed using previously described Huh-7 cells containing subgenomic HCV replicon I₃₇₇/NS3-3'/wt (Huh 9-13) (Lohmann et al., 1999). Cells were cultured in DMEM (Gibco) supplemented with 10% heat-inactivated FCS (Integro, The Netherlands), 1x non-essential amino acids, 100 IU/ml penicillin (Gibco), 100 µg/ml streptomycin (Gibco) and 1 mg/ml Geneticin® (G418; Gibco). Antiviral assays were performed as described before (Delang et al., 2012). Briefly, cells were seeded at a density of 5 x 10³ cells per well in a 96-well cell culture plate in complete DMEM. Following incubation of 24 hours at 37°C, serial dilutions of the test compounds in complete DMEM were added in a total volume of 100 µL. Replicon RNA levels after 3 days of incubation were determined by reverse transcription quantitative polymerase chain reaction (RT-qPCR). Primers used for detection of HCV replicon RNA were: 5'-CCGGCTACCTGCCCATTC-3' (forward primer), 5'-CCAGATCATCCTGATCGACAAG-3' (reverse primer) and 5'-FAM-ACATCGCATCGAGCGAGCACGTAC-TAMRA-3' (probe).

Analysis of viral polyprotein processing *in vivo*

The *in vivo* metabolic labeling was performed as described previously (Lanke et al., 2007). Briefly, BGM cells grown in 24-well plates were infected with CVB3 at MOI 50. After 4 hr incubation at 37 °C cells were starved of methionine and cysteine for 30 min using medium devoid of these amino

acids. Proteins were then labeled for 30 min using ³⁵S-methionine in the presence or absence of compound. At 5 hr p.i. cells were lysed, protein lysates were resolved by SDS-PAGE (10% polyacrylamide), and gels were fixed and analyzed by autoradiography.

Target identification by siRNA sensitization (TISS) assay

TISS assay was performed as previously described (Arita et al., 2011). In short, HEK293 cells in 96-well plates were transfected with siRNA pools by using Lipofectamine RNAiMAX transfection reagent (Invitrogen). At 72 hr post transfection, these cells were infected with 800 infectious units PV pseudovirus and treated with DMSO or 1.25 μM ITZ. Firefly luciferase activity was measured at 7 hr p.i. using Steady-Glo Luciferase Assay System (Promega). The effect of siRNA treatment on the sensitivity to each compound was determined by calculating the normalized PV pseudovirus infection. This number represents the level of firefly luciferase activity for compound-treated and siRNA-transfected cells divided by the firefly luciferase activity measured in siRNA-transfected cells in the absence of compounds.

Rescue experiments

HeLa R19 cells were seeded in 96-well plates and transfected the next day with plasmids encoding full-length human or rabbit OSBP (pEGFP-hOSBP or pcDNA4-His-Max-rOSBP) or ORP4L (pcDNA4-His-Max-ORP4L). After 24hrs of expression, cells were infected with virus, and titers or *Renilla* luciferase values were determined as described under 'Virus infection'.

siRNA knockdown experiments

HeLa R19 cells (2 x 10³ cells/well of a 96-well plate) were reverse transfected with 2 pmol of small interfering RNA (siRNA) per well using Lipofectamine 2000 (Invitrogen) according to the manufacturer's instructions. Scramble siRNA (AllStars Negative Control; Qiagen) was used as a negative control, siRNA against PI4KIIIβ (5'-UGUUGGGGCUUCCUGCCCTT-3') was from Qiagen, and siRNAs against OSBP (two siRNAs mixed at a 1:1 ratio, 2 pmol total per well, 5'-CGCUAAUGGAAGAAGUUUA[dT][dT]-3' and 5'-CCUUUGAGCUGGACCGAAU[dT][dT]-3') and ORP4 (5'-AGAGAUACACAGUCGAAA[dT][dT]-3', 5'-GGCUCGUGGGAUGAACAAA[dT][dT]-3', 5'-GGUUUGCUCUCUUACUACA[dT][dT]-3', and 5'-GCACCUAACUGUUCACAA[dT][dT]-3') were from Sigma. After 48 h, cells were infected with virus described under 'Virus infection', an MTS-assay (essentially as described under 'Multicycle CPE-reduction assay') was performed to evaluate effects of knockdown on cell viability, or RNA was isolated using the Nucleospin RNA kit (Macherey Nagel) and used to evaluate knockdown efficiency by qPCR analysis using the LightCycler 480 SYBR green I Master kit (Roche) (primers used: OSBP 5'-ATCAAACAGGTCAACGAACGAG-3' and 5'-GGGTCTGGGCTAACATGAGGA-3', ORP4 5'-GAACCTGTGTCCGAGACGAC-3' and 5'-CCTGAGCTTGACTCTGACCC-3').

Immunofluorescence microscopy

Microscopic analyses were performed using HeLa R19, BGM or RD cells grown to subconfluency on coverslips in 24-well plates. Where indicated, cells were transfected with plasmids FAPP1-PH-GFP, pEGFP-OSBP, or pEGFP-Golgi (encoding GFP-fused GalT aa1-81; Clontech) using Fugene (Roche) according to the manufacturer's instructions, and after overnight expression the cells were treated with compounds as indicated. In other experiments, cells were infected with CVB3 and in some cases treated with compounds as indicated. Cells were fixed at the indicated time points after addition of the drugs or after infection with 4% paraformaldehyde, permeabilized with PBS/0.1% Triton X-100 (for PI4KIIIβ stainings) or PBS/0.2% saponin/5% BSA (all other experiments), immunostained with antibodies, in some cases DNA was counterstained with Hoechst-33258 or DAPI, and embedded in Mowiol (PolySciences) or FluorSave (Merck). For Filipin staining, cells were fixed and permeabilized with saponin as above, then stained with 25 μg/ml Filipin III (freshly diluted from a 25 mg/ml stock in DMSO) (Sigma) in PBS and embedded in FluorSave. Cells were imaged using standard Leica DMR or Olympus BX60 microscopes, a Leica SPE-II DMI-4000 confocal laser scanning microscope, or a Nikon Ti Eclipse microscope equipped with an Endor DU/897 EMCCD-camera.

To analyze co-localization of OSBP with 3A, images were processed using ImageJ as follows. The a background signal derived from an area without cells was subtracted from the image, single cells were outlined and a mask was created, and all signal outside the mask was cropped to exclude it from the calculations. Manders' co-localization coefficient was calculated using the JACoP plugin (Bolte and Cordelières, 2006) with a manually set threshold.

To quantify the intensity of PI4P staining at ROs, images were first deconvoluted using NIS Advanced Research 4.3 software (Nikon) using 10 iterations, then ImageJ was used for further processing. Infected cells were selected, the 3A channel was thresholded with a fixed value, and the intensity of PI4P staining at the 3A-positive structures was quantified for at least ten cells per condition.

To calculate co-localization of filipin with 3A, images were first deconvoluted using NIS Advanced Research 4.3 software (Nikon) (20 iterations), then ImageJ was used to select infected cells and the Pearson's coefficient of co-localization for at least 15 cells per condition was calculated using the Coloc 2 plugin with default settings.

Live-cell imaging

For live-cell imaging experiments HeLa R19 cells were seeded in compartmentalized CELLview petridishes (Greiner Bio-One) and transfected O/N with pEGFP-hOSBP. Dishes were transferred to a humidified, CO₂- and temperature-controlled chamber (Tokai-Hit) for imaging on a Nikon A1R confocal laser scanning microscope mounted on a Nikon Eclipse-Ti base, cells were selected for imaging and the reference image (t=0) was taken. For the long-term imaging experiment, compounds were added from a two-fold concentrated dilution to the compartments and cells at four different positions per well were imaged O/N. From 0 to 30 min after addition of the drugs, images were taken as fast as possible (i.e. at ~1.5 min intervals), then intervals were gradually increased to 15 min intervals from 2 hr after addition of the compounds onward to prevent bleaching and phototoxicity during the O/N imaging: from 30 to 60 min intervals were 5 min, until 3.5 hr intervals were 15 min and finally intervals were 30 min for the rest of the experiment. Images were processed and quantified using the Nikon NIS-Elements software. For quantification, regions of interest were defined in the perinuclear region where a stronger OSBP signal was observed than in the rest of the cytoplasm (i.e. the Golgi) and the change in average fluorescence intensity in this area was quantified. A movie was assembled using Adobe Premier Pro CS6 software.

In vitro DHE and PI4P transport assays

Previously described liposomal assays (Mesmin et al., 2013) were used to test the sterol and PI4P transfer activities of OSBP (schematically depicted in Figures 6A and 6B, respectively). Briefly, sterol transfer is measured using the fluorescent cholesterol analog dehydroergosterol (DHE). DHE is transferred by OSBP from ER-like liposomes (ER_{like}) covered with VAP-A to Golgi-like liposomes (Golgi_{like}) doped with dansyl-phosphatidylethanolamine (DNS-PE). Upon DHE transfer, there will be Förster resonance energy transfer (FRET) from DHE to DNS-PE due to the close proximity between the two fluorophores. In the PI4P-transfer assay, PI4P is transported by OSBP from Golgi-like liposomes to ER-like acceptor liposomes and detected using a sensor consisting of the FAPP1 PH-domain labeled with the fluorophore NBD (^{NBD}PH). When the sensor is bound to PI4P on the Golgi-like liposomes doped with rhodamine-PE (Rho-PE), NBD fluorescence is quenched by the rhodamine. Upon transfer of PI4P to the ER-like liposomes, the sensor moves from the Golgi-like to the ER-like liposomes and NBD-fluorescence is dequenched.

Egg PC (L- α -phosphatidylcholine), liver PI (L- α -phosphatidylinositol), brain PS (L- α -phosphatidylserine), brain PI4P (L- α -phosphatidylinositol-4-phosphate), Dansyl (DNS)-PE (1,2-dioleoyl-*sn*-glycero-3-phosphoethanolamine-N-(5-dimethylamino-1-naphthalenesulfonyl)), Rhodamine (Rhod)-PE (1,2-dipalmitoyl-*sn*-glycero-3-phosphoethanolamine-N-(lissamine rhodamine B sulfonyl)), DOGS-NTA-Ni²⁺ (1,2-dioleoyl-*sn*-glycero-3-[(N-(5-amino-1-carboxypentyl)iminodiacetic acid)succinyl]) were purchased from Avanti Polar Lipids. Cholesterol and dehydroergosterol (DHE) were from Sigma Aldrich. The concentration of DHE in stock solution in methanol was determined by UV-spectroscopy using an extinction coefficient of 13,000 M⁻¹.cm⁻¹.

Full-length OSBP, VAP-A[8-212]His₆, NBD-PH_{FAPP1} and Arf1 were purified as described previously (Mesmin et al., 2013). To prepare liposomes, lipids from chloroform solutions were mixed at the desired molar ratio, and the solvent was removed in a rotary evaporator. The lipid film was hydrated in 50 mM HEPES pH 7.2 and 120 mM potassium acetate (HK buffer) to give a suspension of large multilamellar liposomes. The suspension was then frozen and thawed five times and extruded through polycarbonate filters of 0.1 μ m pore size using a mini-extruder (Avanti Polar Lipids). Unilamellar liposomes were stored in the dark and used within 2 days. For all transport experiment, ER-like liposomes contain: egg PC/brain PS/DOGS-NTA-Ni²⁺ (93/5/2 mol/mol) and Golgi-like liposomes contain: egg PC/liver PE/brain PS/liver PI/DNS-PE (63.5/19/5/10/2.5 mol/mol).

Fluorescence experiments were performed in a Shimadzu RF-5301-PC spectrofluorimeter. The sample (volume 600 μ l) was placed in a cylindrical quartz cell, continuously stirred with a small

magnetic bar and equilibrated at 37°C. For DHE transfer assays, Golgi-like liposomes with 2.5 mol% DNS-PE (63.3 μM total lipids) were loaded with Arf1.GTP (0.3 μM) and incubated with 1 μM VapA[8-212]His₆ in HKM buffer (HK buffer supplemented with 1 mM MgCl₂) in the presence of 25-OH, ITZ or other azoles (different stock concentration in DMSO, DMSO/buffer final ratio v/v 1/100), prior to the addition of ER-like liposomes supplemented with 18 mol% DHE (63.3 μM total lipids) and of OSBP (100 nM final concentration). The sterol transport activity of OSBP was monitored by FRET between DHE and DNS-PE, measured at 525 nm (bandwidth 5 nm) upon excitation at 310 nm (bandwidth 1.5 nm). Methyl- β -cyclodextrin (1 mM) was used to determine the maximal FRET signal due to full sterol equilibration between ER-like and Golgi-like liposomes. For PI4P transfer assay, Golgi-like liposomes with 2% Rhod-PE (300 μM total lipids) were incubated in HKM buffer with 250 nM NBD-PH_{FAPP}, 3 μM VAP-A[8-212]His₆ in the presence or not of ITZ or other azoles (at different stock concentration, in DMSO). PI4P transport was followed by measuring the NBD emission signal at 510 nm (bandwidth 10 nm) upon excitation at 460 nm (bandwidth 1.5 nm). ER-like liposomes (300 μM lipid) and 100 nM OSBP were sequentially added. Maximal signal corresponding to PI4P equilibration between both types of liposomes was determined by mixing control ER- and Golgi-like liposomes, each containing 1% PI4P.

Liposomal float-up experiments

PH-FFAT (OSBP fragment 76-408) was purified as described (Mesmin et al., 2013), and the flotation experiments were done as previously detailed (Bigay et al., 2005). Briefly, PH-FFAT (0.75 μM) was incubated 5 min at room temperature with 0.75 mM liposomes (ER- or Golgi-like as prepared for the PI4P transfer assay), with or without VAP-A (2 μM) and/or ITZ (1 or 10 μM) as indicated. The suspension (150 μl) was mixed with 100 μl high sucrose solution (30% w/v final sucrose concentration), and overlaid by 200 μl 25% w/v sucrose solution, then by 50 μl buffer without sucrose. The sample was centrifuged at 55,000 rpm in a TLS-55 rotor (Beckman) for 1 hr at 20°C. The bottom (250 μl), middle (150 μl) and top (100 μl) fractions were manually collected from the bottom with a Hamilton syringe. Proteins bound to floating liposomes present in top fractions were analyzed by SDS-PAGE.

OSBP proteolysis

Purified OSBP (3,3 μM) was incubated at 30°C under constant agitation in the presence of 2 $\mu\text{g/ml}$ trypsin, and the reaction was stopped 5 min after trypsin mixture by addition of 2 mM PMSF. Absence of residual full-length protein and accumulation of the ~35kDa ORD fragment [as identified in (Mesmin et al., 2013)] was checked by 15% SDS-PAGE before DHE or PI4P transfer assay.

MicroScale Thermophoresis (MST)

The interaction between ITZ and GFP-hOSBP-SII was investigated by MicroScale Thermophoresis (MST) [see e.g. (Jerabek-Willemsen et al., 2011; Seidel et al., 2013)]. pEGFP-hOSBP-SII was transfected into HEK293T cells using polyethyleimine (PEI) (Polysciences) and after ~5hrs the medium was replaced by expression medium (293SerumFree medium [Gibco] supplemented with GlutaMax [Gibco], 3 g/l Primatone-RL-UF, 2 g/l D-glucose monohydrate, 3.7 g/l NaHCO₃, 1.5% DMSO, 100 U/ml penicillin and 100 $\mu\text{g/ml}$ streptomycin). After two days, cells were harvested by centrifugation, washed with PBS and pelleted again. The cell pellet was snap-frozen in liquid nitrogen and stored at -80°C, or used directly for a purification. Cells were lysed in lysis buffer (50 mM Tris-HCl pH7.4, 250 mM NaCl, 1 mM EDTA, 0.5% nonidet-P40 with protease inhibitor complex [Roche]) for 15 min on ice, centrifuged for 20 min at ~20K \times g, and bound to StrepTactin beads (IBA). Beads were loaded in a column (Bio-Rad), unbound material was drained and beads were washed with washing buffer (50mM Tris-HCl pH7.4, 250 mM NaCl, 1 mM EDTA). Proteins were eluted in elution buffer (washing buffer with 10% glycerol, 2.5mM biotin and protease inhibitor complex), aliquoted, snap-frozen in liquid nitrogen and stored at -80°C. Purity of the protein preparations was checked by SDS-PAGE stained with GelCode Blue (Pierce) and protein concentrations were determined using Bradford reagent (Bio-Rad).

For MST measurements, proteins were thawed on ice, centrifuged for 5 min at full speed in a table top centrifuge to remove any protein aggregates, and diluted in MST buffer (50 mM Tris-HCl pH7.6, 150 mM NaCl, 10 mM MgCl₂) supplemented with 0.05% Tween-20. ITZ was serially diluted in 16 two-fold dilution steps in MST buffer with Tween-20. Protein and ITZ dilutions were mixed, loaded in standard treated capillaries (NanoTemper Technologies) and measured using a NanoTemper Monolith NT.115 instrument (NanoTemper Technologies) equipped with a blue filter set, which is compatible with GFP

fluorescence. Measurements were performed at 22-24°C, 20% MST power, 20% LED power. Individual experiments were analyzed using the NTAanalysis software (NanoTemper Technologies), normalized fluorescence values of individual experiments ($F_{norm}[1/1000]$) were exported to Excel, base-line corrected by subtracting the average of the first three values (lowest ITZ concentrations, plateau for OSBP with no ITZ bound), and normalized to maximal binding using the amplitude calculated for each measurement by the NTAanalysis software. Data of three individual experiments were averaged. Data were plotted and a curve was fitted with the fit function from the law of mass action.

SUPPLEMENTAL FIGURES

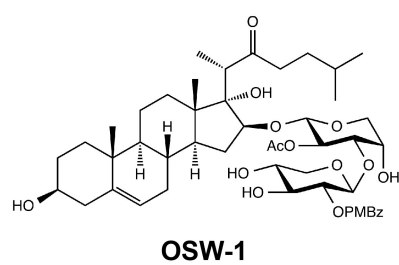
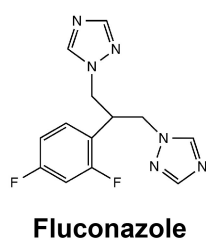
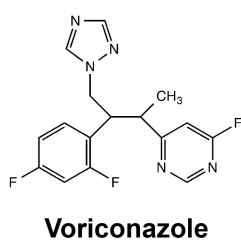
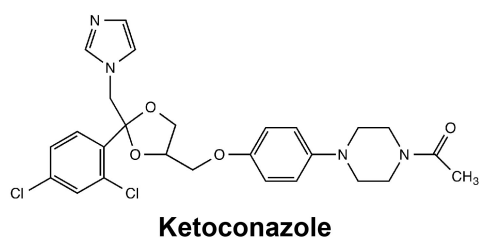
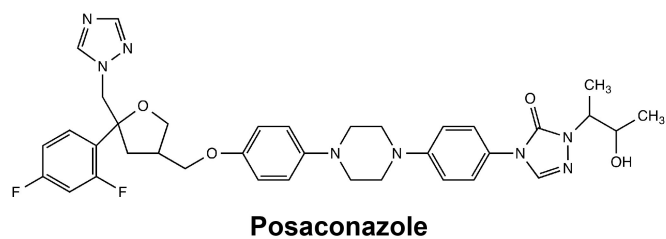
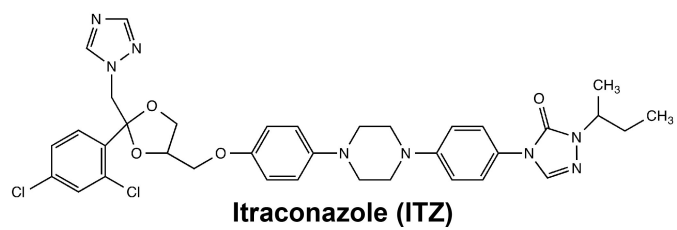


Figure S1. Structural formulae of compounds used, Related to Figures 1-7.

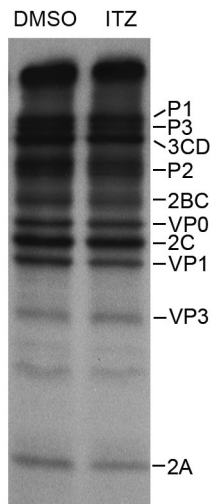


Figure S2. ITZ does not affect viral polyprotein synthesis or processing, Related to Figure 1.

To investigate whether ITZ affected viral polyprotein synthesis or processing, we analyzed viral proteins at 4.5 h p.i. when production of host proteins is severely suppressed because of the virus-induced shut-off of cap-dependent translation. Specifically, BGM cells were infected with CVB3 at MOI 50. At 4 hr p.i., cells were starved for methionine for 30 min and subsequently incubated with [³⁵S]methionine in the presence of DMSO or 25 μ M ITZ for another 30 min. Proteins were analyzed by SDS-PAGE. The levels of viral proteins were similar in the absence or presence of ITZ, indicating that viral polyprotein synthesis and processing were unaffected by ITZ.

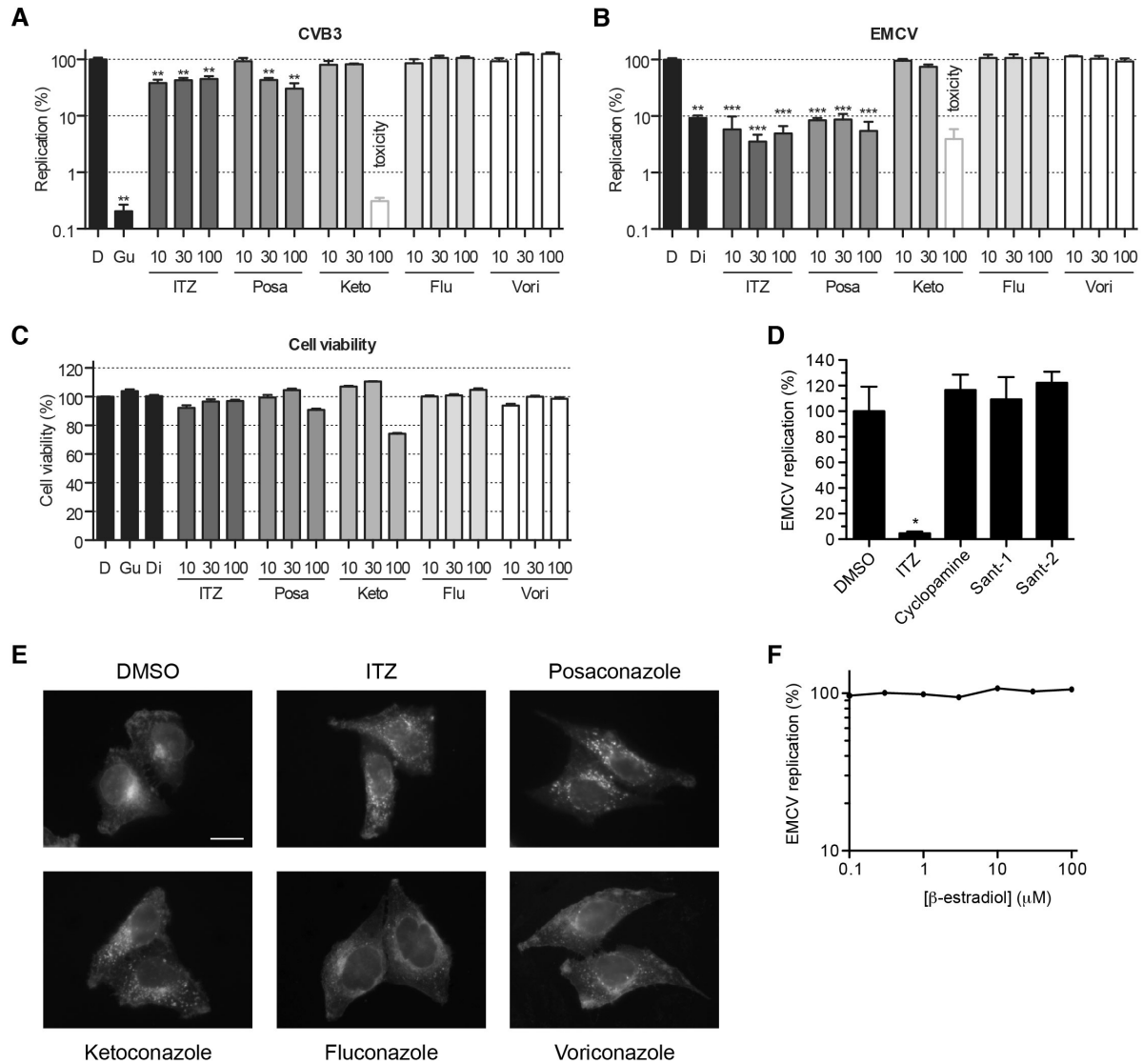


Figure S3. ITZ does not inhibit virus replication through known targets, Related to Figure 2.

(A-C) HeLa R19 cells were infected with RLuc-CVB3 (A) or RLuc-EMCV (B), treated with antifungal azoles as in Figure 2, and *Renilla* luciferase levels were measured after 7 hr. Acute toxicity of the drug treatments was analyzed in parallel using an MTS assay as in Figure 1B (C). The toxicity of treatment with 100 μM ketoconazole prevents drawing a conclusion about any antiviral effect of this drug concentration on CVB3. (D) HeLa R19 cells were infected with RLuc-EMCV, treated with Hedgehog pathway antagonists as in Figure 2, and *Renilla* luciferase levels were measured after 6 hr. (E) HeLa R19 cells were treated with 10 μM antifungal azoles for 6 hr, fixed and cholesterol was stained with filipin. Cholesterol was redistributed only by ITZ, posaconazole and ketoconazole, but not by fluconazole or voriconazole. (F) HeLa R19 cells were infected with RLuc-EMCV, treated with β-estradiol as in Figure 2, and *Renilla* luciferase levels were measured after 6 hr. Scale bars correspond to 10 μm. Asterisks indicate statistical significance compared to the DMSO control. D, DMSO; Gu, Guanidine HCl (known replication inhibitor of CVB3); Posa, posaconazole; Keto, ketoconazole; Flu, fluconazole; Vori, voriconazole.

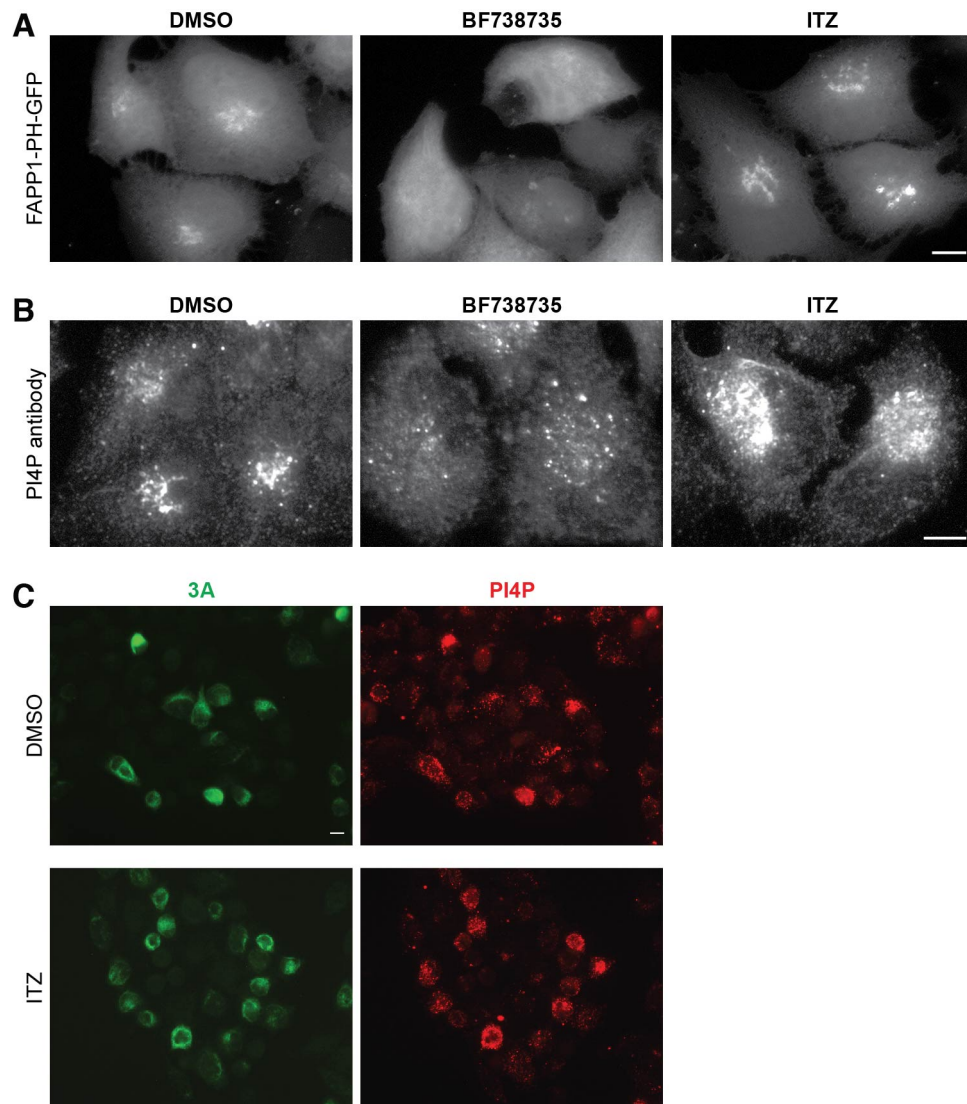


Figure S4. ITZ does not inhibit PI4KIII β in control or CVB3-infected cells, Related to Figure 2.

(A) HeLa cells stably expressing the PI4P-sensor FAPP1-PH-GFP were treated with DMSO, 1 μ M BF738735 (PI4KIII β inhibitor), or 10 μ M ITZ for 2.5 hr, fixed and processed for microscopy. (B) HeLa R19 cells were treated as in (B), fixed and stained with an antibody against PI4P. (C) ITZ does not inhibit PI4P accumulation in infected cells. HeLa R19 cells were infected with CVB3 at MOI 10 and immediately after infection treated with DMSO or 10 μ M ITZ, which does not fully inhibit replication. At 5 hr p.i., the cells were fixed and stained with antibodies against 3A and PI4P. Scale bars correspond to 10 μ m.

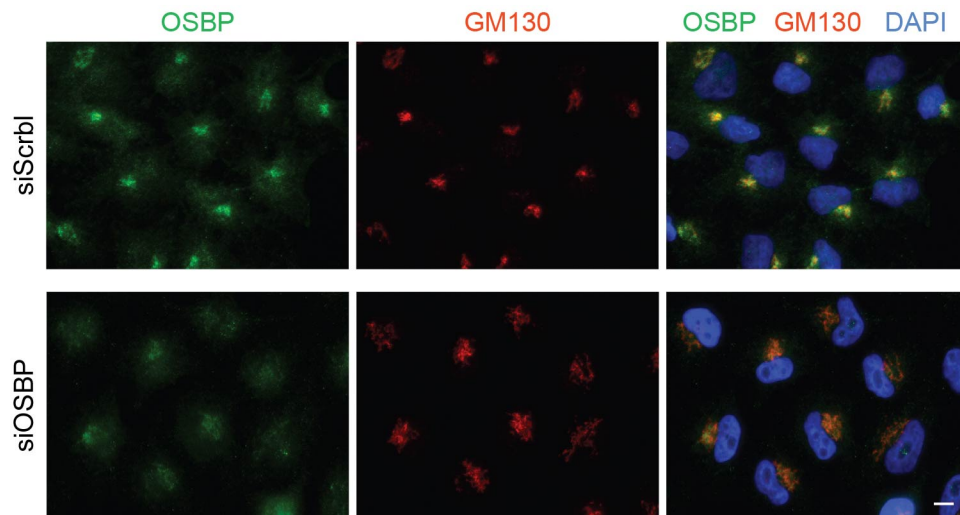


Figure S5. OSBP knockdown decreased OSBP at the protein level, Related to Figure 3.

HeLa R19 cells were transfected with siRNA against OSBP or a scrambled siRNA as a negative control as in Figure 3D. After 48 hr, cells were fixed and immunostained for OSBP and GM130 as Golgi marker, and nuclei were counterstained with DAPI. Knockdown of OSBP at the protein level is evident by a weaker OSBP staining both on Golgi structures and throughout the cytoplasm. Of note, OSBP knockdown caused the Golgi to become less compact, which at the same time demonstrates that knockdown was efficient enough to induce a physiological effect. The scale bar corresponds to 10 μm .

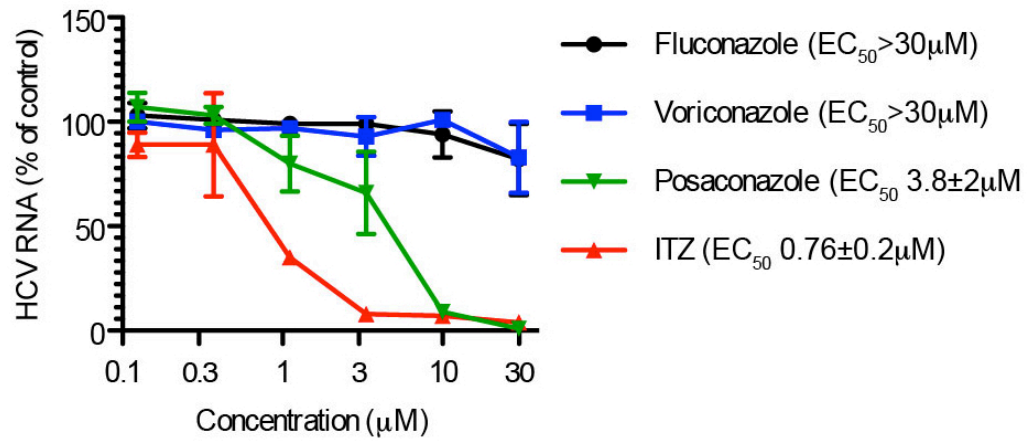


Figure S6. ITZ and posaconazole inhibit HCV replication, Related to Figure 3.

Huh 9-13 cells carrying a HCV genotype 1b subgenomic replicon were treated with ITZ or other antifungal azoles and replication was determined after 3 days by Q-PCR. Values are plotted as % of untreated control (UTC), experiments were performed in triplicates and mean \pm SEM are plotted. EC₅₀ values are means \pm SD from an experiment performed in triplicate. For all compounds, 50% cytotoxic concentrations (CC₅₀) were >30 μ M (data not shown).

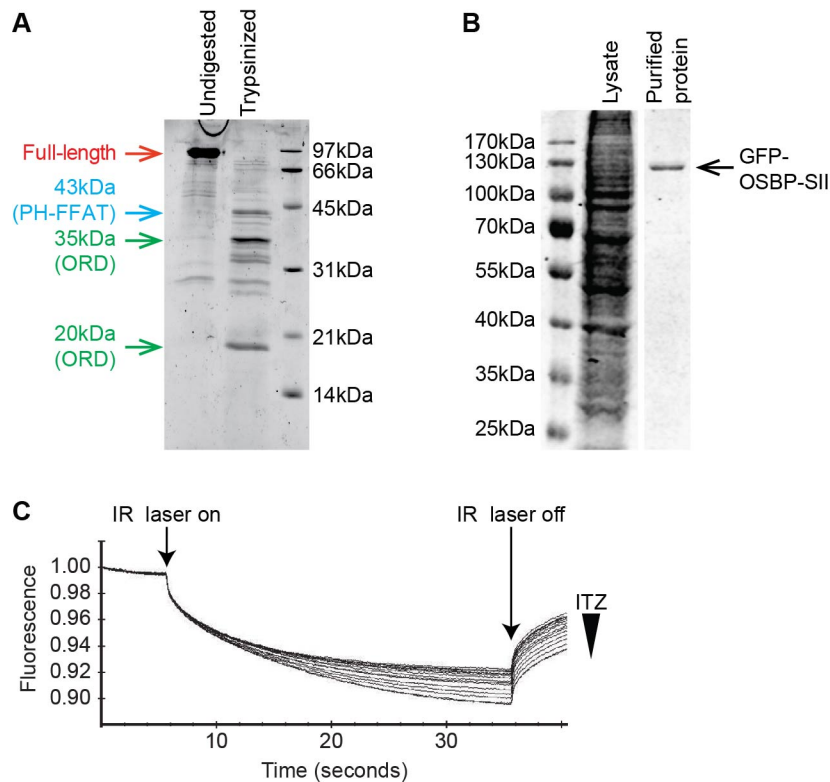


Figure S7. Limited trypsinization of OSBP, purification of GFP-OSBP-SII and thermophoretic curves of ITZ-binding to GFP-OSBP-SII, Related to Figure 5.

(A) Purified full-length OSBP was subjected to limited trypsinization for 5 min. Protein fragments were separated by SDS-PAGE and stained using coomassie. Full-length (~100 kDa) OSBP was cleaved into a ~43 kDa fragment, which corresponds to an N-terminal part comprising the PH-domain and the FFAT-motif, and two fragments of ~35 kDa and ~20 kDa, which are derived from the ORD and which retain the lipid transfer activities (Mesmin et al., 2013). (B) GFP-OSBP-SII was expressed in HEK293T cells and purified using StrepTactin beads. Cell lysate from a typical GFP-OSBP-SII expression and purified protein were analyzed by SDS-PAGE and the gel was stained using GelCode Blue (Pierce). (C) Thermophoretic curves of a representative MicroScale Thermophoresis experiment to investigate the interaction between ITZ and GFP. Each of the 16 curves represents the thermophoretic behavior of GFP-OSBP-SII with a different concentration of ITZ. All curves are from the same measurement.

SUPPLEMENTAL MOVIE LEGENDS

Supplemental Movie 1. ITZ and OSW-1 induce a fast relocalization of OSBP, Related to Figure 4.

HeLa R19 cells transfected with GFP-OSBP and treated with DMSO, 10 μ M of ITZ or 10 nM OSW-1 were imaged O/N by live-cell confocal laser scanning microscopy. During the first 30 minutes, images were taken as fast as possible (~1.5 minute intervals), then intervals were stepwise increased to 30 min from 3.5 hr onward. Representative groups of cells are shown. The time after addition of the compounds for each image is indicated as hr : min : sec. The size of the scale bar corresponds to 10 μ m.

SUPPLEMENTAL TABLE

Table S1. Antiviral activity of itraconazole in a low MOI multi-cycle CPE-reduction assay, Related to Figure 1.

Virus	Species	Cell line	EC₅₀¹
<i>Enterovirus</i> ²			
EV71	EV-A	BGM	0.30 ± 0.02
CVA16	EV-A	Hela H	0.06 ± 0.01
CVB3	EV-B	Vero	0.79 ± 0.06
ECHO11	EV-B	BGM	0.50 ± 0.05
CVA21	EV-C	Hela R19	0.77 ± 0.11
PV1	EV-C	BGM	1.23 ± 0.59
PV2	EV-C	BGM	1.54 ± 0.02
PV3	EV-C	BGM	0.83 ± 0.09
EV68	EV-D	Hela R19	0.43 ± 0.07
EV70	EV-D	Hela R19	0.92 ± 0.06
HRV14	HRV-B	Hela R19	0.64 ± 0.08
<i>Cardiovirus</i> ²			
Mengovirus	EMCV	BGM	0.57 ± 0.02
<i>Aphthovirus</i> ²			
ERAV-1	ERAV	BGM	>80
<i>Parechovirus</i> ²			
HPeV-1	HPeV	HT-29	>80

¹ Mean values calculated from at least three experiments ± SD. The cytotoxicity values (CC50) were >100 µM for all cell lines, although cell viability readings were somewhat decreased at higher concentrations, which seemed to be mainly due to an effect on cell proliferation rather than cytotoxicity (not shown).

² Genera to which the viruses belong are italicized.

SUPPLEMENTAL REFERENCES

- Aminev, A.G., Amineva, S.P., and Palmenberg, A.C. (2003). Encephalomyocarditis virus (EMCV) proteins 2A and 3BCD localize to nuclei and inhibit cellular mRNA transcription but not rRNA transcription. *Virus Res.* *95*, 59-73.
- Arita, M., Kojima, H., Nagano, T., Okabe, T., Wakita, T., and Shimizu, H. (2011). Phosphatidylinositol 4-kinase III beta is a target of enviroxime-like compounds for antipoliiovirus activity. *J. Virol.* *85*, 2364-2372.
- Arita, M., Nagata, N., Sata, T., Miyamura, T., and Shimizu, H. (2006). Quantitative analysis of poliomyelitis-like paralysis in mice induced by a poliovirus replicon. *J. Gen. Virol.* *87*, 3317-3327.
- Arita, M., Wakita, T., and Shimizu, H. (2009). Cellular kinase inhibitors that suppress enterovirus replication have a conserved target in viral protein 3A similar to that of enviroxime. *J. Gen. Virol.* *90*, 1869-1879.
- Balla, A., Tuymetova, G., Tsiomenko, A., Varnai, P., and Balla, T. (2005). A plasma membrane pool of phosphatidylinositol 4-phosphate is generated by phosphatidylinositol 4-kinase type-III alpha: studies with the PH domains of the oxysterol binding protein and FAPP1. *Mol. Biol. Cell* *16*, 1282-1295.
- Bigay, J., Casella, J.F., Drin, G., Mesmin, B., and Antonny, B. (2005). ArfGAP1 responds to membrane curvature through the folding of a lipid packing sensor motif. *EMBO J.* *24*, 2244-2253.
- Bolte, S., and Cordelieres, F.P. (2006). A guided tour into subcellular colocalization analysis in light microscopy. *J. Microsc.* *224*, 213-232.
- Carette, J.E., Raaben, M., Wong, A.C., Herbert, A.S., Obernosterer, G., Mulhkar, N., Kuehne, A.I., Kranzusch, P.J., Griffin, A.M., Ruthel, G., *et al.* (2011). Ebola virus entry requires the cholesterol transporter Niemann-Pick C1. *Nature* *477*, 340-U115.
- De Palma, A.M., Thibaut, H.J., Van der Linden, L., Lanke, K., Heggermont, W., Ireland, S., Andrews, R., Arimilli, M., Al-Tel, T.H., De Clercq, E., *et al.* (2009). Mutations in the nonstructural protein 3A confer resistance to the novel enterovirus replication inhibitor TTP-8307. *Antimicrob. Agents Chemother.* *53*, 1850-1857.
- Delang, L., Vliegen, I., Leyssen, P., and Neyts, J. (2012). In vitro selection and characterization of HCV replicons resistant to multiple non-nucleoside polymerase inhibitors. *J. Hepatol.* *56*, 41-48.
- Dorobantu, C.M., Van der Schaar, H.M., Ford, L.A., Strating, J.R., Ulferts, R., Fang, Y., Belov, G., and Van Kuppeveld, F.J. (2014). Recruitment of PI4KIIIbeta to Coxsackievirus B3 replication organelles is independent of ACBD3, GBF1, and Arf1. *J. Virol.* *88*, 2725-2736.
- Jerabek-Willemsen, M., Wienken, C.J., Braun, D., Baaske, P., and Duhr, S. (2011). Molecular interaction studies using microscale thermophoresis. *Assay Drug. Dev. Technol.* *9*, 342-353.
- Lanke, K., Krenn, B.M., Melchers, W.J., Seipelt, J., and Van Kuppeveld, F.J. (2007). PDTC inhibits picornavirus polyprotein processing and RNA replication by transporting zinc ions into cells. *J. Gen. Virol.* *88*, 1206-1217.
- Lanke, K.H., Van der Schaar, H.M., Belov, G.A., Feng, Q., Duijsings, D., Jackson, C.L., Ehrenfeld, E., and Van Kuppeveld, F.J. (2009). GBF1, a guanine nucleotide exchange factor for Arf, is crucial for coxsackievirus B3 RNA replication. *J. Virol.* *83*, 11940-11949.
- Lohmann, V., Korner, F., Koch, J., Herian, U., Theilmann, L., and Bartenschlager, R. (1999). Replication of subgenomic hepatitis C virus RNAs in a hepatoma cell line. *Science* *285*, 110-113.
- Mesmin, B., Bigay, J., Moser von Filseck, J., Lacas-Gervais, S., Drin, G., and Antonny, B. (2013). A four-step cycle driven by PI(4)P hydrolysis directs sterol/PI(4)P exchange by the ER-Golgi tether OSBP. *Cell* *155*, 830-843.
- Seidel, S.A., Dijkman, P.M., Lea, W.A., van den Bogaart, G., Jerabek-Willemsen, M., Lazic, A., Joseph, J.S., Srinivasan, P., Baaske, P., Simeonov, A., *et al.* (2013). Microscale thermophoresis quantifies biomolecular interactions under previously challenging conditions. *Methods* *59*, 301-315.
- Suchanek, M., Hynynen, R., Wohlfahrt, G., Lehto, M., Johansson, M., Saarinen, H., Radzikowska, A., Thiele, C., and Olkkonen, V.M. (2007). The mammalian oxysterol-binding protein-related proteins (ORPs) bind 25-hydroxycholesterol in an evolutionarily conserved pocket. *Biochem. J.* *405*, 473-480.
- Van der Schaar, H.M., Van der Linden, L., Lanke, K.H., Strating, J.R., Purstinger, G., De Vries, E., De Haan, C.A., Neyts, J., and Van Kuppeveld, F.J. (2012). Coxsackievirus mutants that can bypass host factor PI4KIIIbeta and the need for high levels of PI4P lipids for replication. *Cell Res.* *22*, 1576-1592.
- Van Ooij, M.J., Vogt, D.A., Paul, A., Castro, C., Kuijpers, J., Van Kuppeveld, F.J., Cameron, C.E., Wimmer, E., Andino, R., and Melchers, W.J. (2006). Structural and functional characterization of the coxsackievirus B3 CRE(2C): role of CRE(2C) in negative- and positive-strand RNA synthesis. *J. Gen. Virol.* *87*, 103-113.
- Wessels, E., Duijsings, D., Niu, T.K., Neumann, S., Oorschot, V.M., De Lange, F., Lanke, K.H., Klumperman, J., Henke, A., Jackson, C.L., *et al.* (2006). A viral protein that blocks Arf1-mediated COP-I assembly by inhibiting the guanine nucleotide exchange factor GBF1. *Dev. Cell* *11*, 191-201.

Wessels, E., Duijsings, D., Notebaart, R.A., Melchers, W.J., and Van Kuppeveld, F.J. (2005). A proline-rich region in the coxsackievirus 3A protein is required for the protein to inhibit endoplasmic reticulum-to-golgi transport. *J. Virol.* 79, 5163-5173.

Zoll, J., Erkens Hulshof, S., Lanke, K., Verduyn Lunel, F., Melchers, W.J.G., Schoondermark-van de Ven, E., Roivainen, M., Galama, J.M.D., and van Kuppeveld, F.J.M. (2009). Saffold Virus, a human Theiler's-like cardiovirus, is ubiquitous and causes infection early in life. *PLoS Path.* 5, e1000416.